Journal of Helminthology

cambridge.org/jhl

A new species of *Physaloptera* (Nematoda: Spirurida) from *Proechimys gardneri* (Rodentia: Echimyidae) from the Amazon rainforest and molecular phylogenetic analyses of the genus

A. Maldonado Jr[1], R.O. Simões[1,2], J. São Luiz[1], S.F. Costa-Neto[1,3] and R.V. Vilela[1]

[1]Laboratório de Biologia e Parasitologia de Mamíferos Silvestres Reservatórios, FIOCRUZ, Rio de Janeiro, RJ, Brazil; [2]Departamento de Parasitologia Animal, Universidade Federal Rural do Rio de Janeiro, Seropédica, RJ, Brazil and [3]FIOCRUZ da Mata Atlântica, FIOCRUZ, Brazil

Research Paper

Cite this article: Maldonado Jr A, Simões RO, Luiz JS, Costa-Neto SF, Vilela RV (2020). A new species of *Physaloptera* (Nematoda: Spirurida) from *Proechimys gardneri* (Rodentia: Echimyidae) from the Amazon rainforest and molecular phylogenetic analyses of the genus. *Journal of Helminthology* **94**, e68, 1–11. https://doi.org/10.1017/S0022149X19000610

Received: 4 January 2019
Accepted: 26 June 2019

Key words:
Brazil; nematode; rodent

Author for correspondence:
R.O. Simões, E-mail: raquel83vet@gmail.com

Abstract

Nematodes of the genus *Physaloptera* are globally distributed and more than 100 species are known. Their life cycle involves insects, including beetles, cockroaches and crickets, as intermediate hosts. This study describes a new species of *Physaloptera* and reports molecular phylogenetic analyses to determine its relationships within the family Physalopteridae. *Physaloptera amazonica* n. sp. is described from the stomach of the caviomorph rodent *Proechimys gardneri* collected in the Amazon rainforest in the state of Acre, Brazil. The species is characterized by the male having the first and second pair of sessile papillae asymmetrically placed, lacking a median papilla-like protuberance between the third pairs of sessile papillae, differentiated by size and shape of the spicules, while females have four uterine branches. For both nuclear 18S rRNA and MT-CO1 gene-based phylogenies, we recovered *Turgida* sequences forming a clade nested within *Physaloptera*, thus making *Physaloptera* paraphyletic to the exclusion of *Turgida*, suggesting that the latter may have evolved from the former monodelphic ancestral state to a derived polydelphic state, or that some species of *Physaloptera* may belong to different genera. Relationships between most taxa within *Physaloptera* were poorly resolved in our phylogenies, producing multifurcations or a star phylogeny. The star-like pattern may be attributed to evolutionary processes where past simultaneous species diversification events took place. *Physaloptera amazonica* n. sp. formed an independent lineage, separately from the other species of *Physaloptera*, thus supporting the status of a new species. However, all molecular data suggested a closer relationship with other Neotropical species. In conclusion, we added a new species to this already largely diverse genus *Physaloptera*, bringing new insights to its phylogenetic relationships. Further analyses, adding more species and markers, should provide a better understanding of the evolutionary history of physalopterids.

Introduction

Nematodes of the genus *Physaloptera* Rudolphi, 1819 are globally distributed and more than 100 species are known (Pereira *et al.*, 2014; São Luiz *et al.*, 2015). They infect amphibians, reptiles, birds and mammals (Ortlepp, 1922; Chabaud, 1975; Anderson *et al.*, 2009). Their life cycle involves insects, including beetles, cockroaches and crickets, as intermediate hosts (Hobmaier, 1941; Goldberg & Bursey, 2002). The adult worms firmly attach to the stomach wall, where they feed on the mucosa and cause gastritis, enteritis and excessive mucous secretion by the host (Panti-May *et al.*, 2015).

The genus *Proechimys* of caviomorph rodents belongs to the family Echimyidae, which stands out for its extraordinary ecomorphological diversity (Galewski *et al.*, 2005). *Proechimys* is the most speciose and geographically widespread genus of echimyids (Patton & Leite, 2015). These species have terrestrial, nocturnal and solitary habits, although they are often the most abundant non-volant mammals in lowland Neotropical forests (Emmons & Feer, 1997). *Proechimys gardneri* da Silva, 1998 inhabits the Amazon rainforest and is distributed from its eastern limit at the Madeira and Solimões Rivers to its northern limit in a small stretch of the Amazon River (Eler *et al.*, 2012).

Amazonia is the largest and most diverse of the tropical forest wilderness areas (Silva *et al.*, 2005). The Amazon biome is situated in the north of South America, distributed in parts of nine countries: Brazil, Venezuela, Colombia, Peru, Bolivia, Ecuador, Suriname, Guyana and French Guiana (Portal Amazônia, 2018). Sixty per cent of the Amazon rainforest lies in Brazilian territory (Migueis, 2001). However, there are few studies in this region, especially regarding helminth biodiversity.

CAMBRIDGE UNIVERSITY PRESS

In this study, we describe a new species of *Physaloptera* found in the echimyid rodent *P. gardneri* collected in the Brazilian Amazon rainforest in the state of Acre. Additionally, we describe molecular phylogenetic analyses of the new species and representatives of *Physaloptera* and other physalopteroid genera in order to determine its relationships within the genus.

Material and methods

Study area

Nematodes were collected from the stomach of five naturally infected *P. gardneri* specimens in the municipality of Xapuri (10°49′S, 68°21′W), Acre, Brazil. Collections were carried out between March 2014 and December 2015, using Tomahawk® (Tomahawk Live Trap, USA)(model 201; 16 × 5 × 5 inches or 40.6 × 12.7 × 12.7 cm) and Sherman® (Sherman Live Trap, USA) (model XLK; 3 × 3.75 × 12 inches or 7.6 × 9.5 × 30.5 cm) live traps. This study was approved by the ethics committee of the Oswaldo Cruz Foundation/FIOCRUZ (CEUA number LW-39/14). Capture and sampling of small mammals were authorized by the Chico Mendes Institute for Conservation of Biodiversity (ICMBIO/SISBIO, license number 13373). For euthanasia, the animals were heavily anaesthetized with an intramuscular injection of thiopental sodium, followed by intracardiac administration of potassium chloride, under the supervision of a licensed veterinarian (Gannon & Sikes, 2011). Parasites were washed in 0.9% NaCl solution and fixed in hot alcohol-formalin-acetic acid (AFA) (2% glacial acetic acid, 3% formaldehyde and 95% ethanol) for morphological identification, or alternatively preserved in 70% ethanol for DNA isolation.

The nematodes were clarified in 80% phenol and mounted on temporary slides. Morphological analyses were conducted using an Olympus BX-51 light microscope (Tokyo, Japan) and images were captured using an Olympus DP-12 digital camera (Tokyo, Japan). Drawings were made using a drawing tube attached to a Nikon Y-IDT light microscope (Tokyo, Japan). Measurements were taken in millimetres (means are followed by the range in parentheses) from eight male and ten female adult specimens. Nematode identification was according to Ortlepp (1922), Vicente *et al.* (1997) and Anderson *et al.* (2009). Holotype, allotype and paratypes were deposited in the Helminthological Collection of the Oswaldo Cruz Institute, Rio de Janeiro (CHIOC).

For scanning electron microscopy analysis, nematodes were washed in 0.1 M Na-cacodylate buffer, pH 7.2, post-fixed in 1% OsO_4 and 0.8% $K_3Fe(CN)_6$, dehydrated in graded ethanol (30–100%) for 2 h and dried by the critical point method with CO_2 (CPD 030, Balzers, Switzerland). The samples were mounted on aluminium stubs, coated with a 20 nm layer of gold and examined with a Jeol JSM 6390LV scanning electron microscope (operating at 15 kV) (JEOL, Akishima, Tokyo, Japan) at the Rudolf Barth Electron Microscopy Platform of Oswaldo Cruz Institute, RJ.

DNA isolation, polymerase chain reaction (PCR) and sequencing

Genomic DNA samples were isolated from two individual nematodes using the Qiagen QIAamp DNA Mini Kit, according to the manufacturer's protocol. DNA amplification by PCR was conducted using designed primers PHYSA_F (5′ GCGAACG GCTCATTATAA 3′) and PHYSA_R (5′ AATTTCACCTCT CAGCA 3′) for a partial region of the nuclear small subunit ribosomal RNA (18S) gene. For the barcode region of the mitochondrial cytochrome *c* oxidase subunit I (MT-CO1) gene, we used the primer cocktail described by Prosser *et al.* (2013). Reactions were carried out in a total volume of 50 µl, containing 33.8 µl of water, 5 µl of 10X buffer (200 mM Tris-HCl (pH 8.4), 500 mM KCl), 3 µl of 50 mM $MgCl_2$, 5 µl of 10 mM dNTP mix, 1 µl of each 10 µM primer, 0.2 µl of 5 U/µl Taq DNA polymerase and 1 µl of DNA sample. Thermal cycling conditions were 95°C for 2 min, followed by 39 cycles at 95°C for 30 s, 54°C for 30 s, 72°C for 1 min and a final extension at 72°C for 1 min. The resulting amplicons were visualized on 1% agarose gel, stained with GelRed, under ultraviolet light after electrophoresis. Successfully amplified products were purified using the QIAquick PCR Purification Kit (Qiagen).

Sequencing reactions and readings were performed at the subunit RPT01A – DNA Sequencing of the Genomic Platform, Technological Platforms Network, Fiocruz (PDTIS/FIOCRUZ), using the Big Dye Terminator v3.1 Cycle Sequencing Kit (Applied Biosystems, USA), on both strands, with the primers mentioned above. Fragments were assembled into contigs and edited for errors and ambiguities with the Geneious 9.1.8 suite (https://www.geneious.com) (Kearse *et al.*, 2012), resulting in consensus sequences. All sequences obtained in this study were deposited in the GenBank database under the accession numbers indicated in table 1.

Phylogenetic tree reconstructions

We conducted phylogenetic analyses using two different datasets, one for the 18S gene and one for the MT-CO1 gene. We sequenced 11 nematode specimens for the partial 18S and MT-CO1 genes. Datasets consisted, along with our specimens, of sequences of other physalopterids retrieved from the GenBank. As outgroups, sequences of *Gnathostoma turgidum* were added to both matrices (table 1). The resulting 18S dataset had 24 taxa, whereas the MT-CO1 dataset had 20 taxa.

Alignments for the 18S gene sequences were produced using the SILVA (high-quality ribosomal RNA databases) online Incremental Aligner (SINA v1.2.11) (Pruesse *et al.*, 2012), whereas alignments for the MT-CO1 gene sequences were produced using the Translator X server (Abascal *et al.*, 2010). Initial alignment for Translator X was provided using MUSCLE (Edgard, 2004). Resulting alignments were edited and trimmed of regions with poor overlap using the Mesquite Version 3.51 (Maddison & Maddison, 2018) software package. Uncorrected pairwise *p*-distances were calculated for each matrix using the program PAUP*, version 4.0a165 (Swofford, 2002).

Phylogenetic reconstructions using maximum parsimony (MP), as optimality criterion, were carried out using PAUP*. The parsimony settings were: collapse branches if the minimum length is zero ('amb-') and treatment of gaps as 'new state' (fifth base); all other parsimony and heuristic search settings were defaults. Branch supports were assessed by nonparametric bootstrap percentages (MP-BS) after 10,000 pseudo replications.

Phylogenetic reconstructions using maximum likelihood (ML), as optimality criterion, were carried out using the program FastTree 2.1 (Price *et al.*, 2010) using the general time reversible (GTR) + G model to optimize the ML. Branch supports were assessed by local support values using the Shimodaira–Hasegawa test (ML-SH) with 1000 resamples. The best-fit nucleotide evolutionary model was calculated under the corrected Akaike information criterion using the Automated Model Selection on PAUP*.

https://doi.org/10.1017/S0022149X19000610 Published online by Cambridge University Press

Table 1. Specimens included in the molecular analyses associated with their GenBank accession numbers for the MT-CO1 and 18S genes, hosts and locality.

Species	18S	MT-CO1	Host	Locality
Gnathostoma turgidum	KT894809	KT894798	*Didelphis aurita*	Brazil
Heliconema longissimum	JF803926	GQ332423	*Anguilla japonica*	Japan
Heliconema longissimum 1	JF803949	–	*Anguilla* sp.	Madagascar
Physalopteridae sp. 1	–	KC130708	*Imantodes* sp.	Mexico
Physalopteridae sp. 2	–	KC130709	*Sceloporus* sp.	Mexico
Physalopteroides sp.	KP338605	–	*Hemidactylus brooki*	India
Physaloptera sp. 1	–	KC130690	*Trimorphodon biscutatus*	Mexico
Physaloptera sp. 2	–	KC130696	*Trimorphodon biscutatus*	Mexico
Physaloptera sp. 3	–	KC130694	*Trimorphodon biscutatus*	Mexico
Physaloptera sp. 4	MG808040	MG808042	*Cebus capucinus*	Costa Rica
Physaloptera sp. 5	–	LC381943	*Colinus virginianus*	USA
Physaloptera sp.6	HM067978	–	*Macaca fascicularis*	China
Physaloptera sp. 7	EF180065	–	*Mephitis*	USA
Physaloptera mirandai 1	KT894815	KP981418	*Metachirus nudicaudatus*	Brazil
Physaloptera mirandai 2	KT894816	KT894805	*Metachirus nudicaudatus*	Brazil
Physaloptera mirandai 3	–	KT894804	*Metachirus nudicaudatus*	Brazil
Physaloptera amazonica n. sp.	MK312472	MK309356	*Proechimys gardneri*	Brazil
Physaloptera bispiculata	KT894817	KT894806	*Nectomys squamipes*	Brazil
Physaloptera galvaoi	KT894818	KT894807	*Cerradomys subflavus*	Brazil
Physaloptera retusa	KT894814	KT894803	*Tupinambis teguixin*	Brazil
Physaloptera thalacomys	–	JF934734	*Perameles gunnii*	Australia
Physaloptera apivori	–	EU004817	*Pernis apivorus*	Germany
Physloptera alata	–	AY702703	*Accipiter gentilis*	Germany
Proleptus obtusus 1	KY411575	KY411568	*Scyliorhinus canicula*	Portugal
Proleptus obtusus 2	–	Ky411574	*Scyliorhinus canicula*	Portugal
Proleptus sp.	JF9347733	–	*Trygonorrhina fasciata*	Australia
Protospirura numidica 1	KT894811	KT894800	*Oxymycterus delator*	Brazil
Protospirura numidica 2	KT894812	KT894801	*Oxymycterus delator*	Brazil
Turdida turgida 1	KT894819	KT894808	*Didelphis aurita*	Brazil
Turdida turgida 2	DQ503459	–	*Didelphis virginiana*	USA
Turdida turgida 3	KP208673	–	*Didelphis aurita*	Brazil
Turgida sp.	–	KC130680	*Didelphis virginiana*	Mexico
Turgida torresi	EF180069	–	*Dasyprocta punctata*	Costa Rica
Spirocerca lupi	AY751497	KC305876	*Canis familiaris*	China

Bayesian phylogenetic inferences (BIs) were carried out using MrBayes version 3.2.6 (Ronquist *et al.*, 2012) in XSEDE using the CIPRES Science Gateway (Miller *et al.*, 2010). To account for different evolutionary processes at each codon position of the MT-CO1 gene, Bayesian analyses were performed using a distinct GTR + I + G model per codon position, with unlinking of base frequencies, GTR and parameters. The 18S gene Bayesian analyses were performed using a single GTR + I + G model. Markov chain Monte Carlo samplings for each matrix were performed for 10,000,000 generations with four simultaneous chains in two runs. We assessed branch supports in Bayesian trees by Bayesian posterior probabilities (BPPs), calculated from trees that were sampled every 100 generations, after the removal of a burn-in fraction of 25%. We assessed the robustness of sampling using the Tracer v1.7.1 program (Rambaut *et al.*, 2018) to calculate the effective sample sizes (ESSs) of parameters. After removal of a burn-in fraction of 25%, values above 100 effectively independent samples were considered sufficiently sampled.

The substitution saturation in each dataset was assessed as proposed by Xia *et al.* (2003) and Xia & Lemey (2009), using the program DAMBE, version 7.0.35 (Xia, 2018). Each codon position was also tested separately in the MT-CO1 dataset. We also tested each dataset for the presence of a phylogenetic signal using the g1 statistic (Sokal & Rohlf, 1995), examining 10,000,000 randomly

https://doi.org/10.1017/S0022149X19000610 Published online by Cambridge University Press

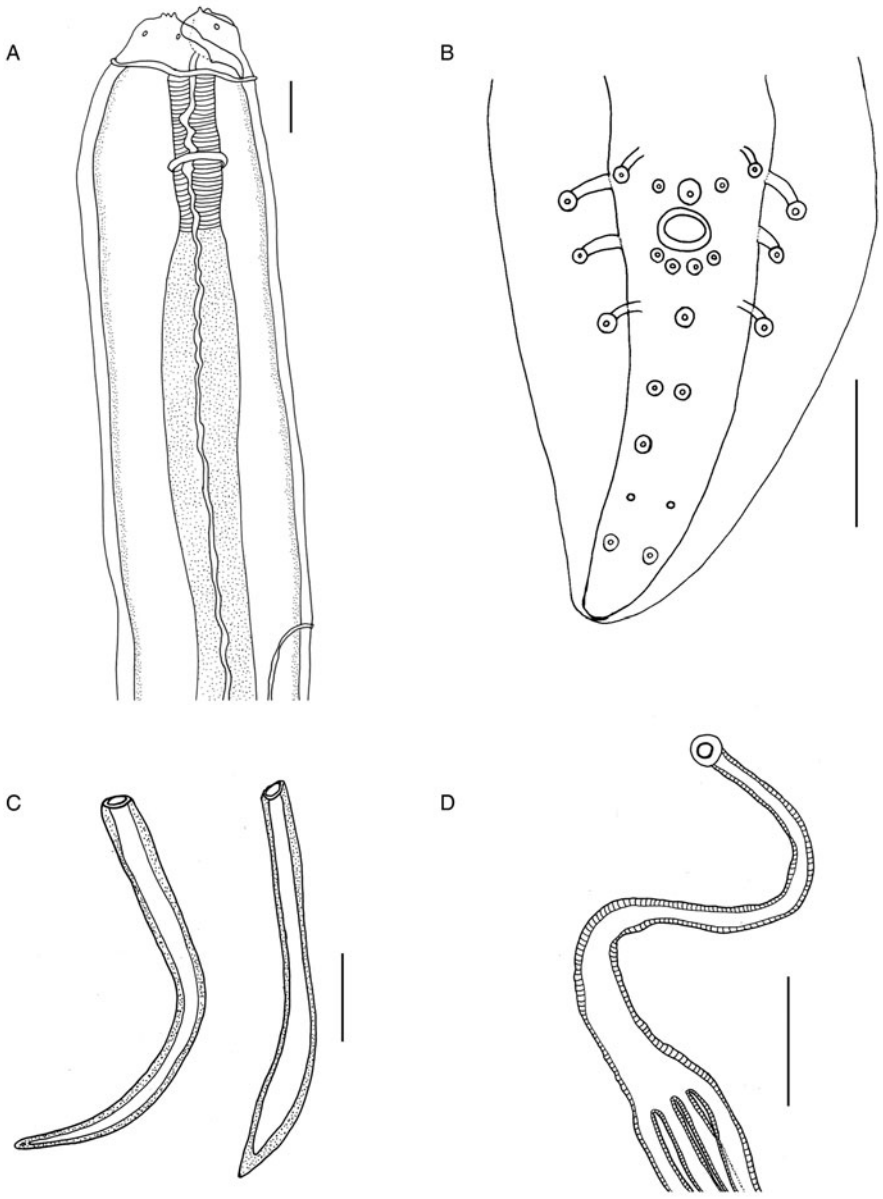

Fig. 1. *Physaloptera amazonica* n. sp. (A) Male, lateral view, anterior end showing tripartite tooth, cephalic papillae, collarette, muscular and glandular oesophagus, nerve ring and excretory pore. (B) Male, ventral view, posterior end with four pairs of pedunculated papillae and 13 sessile papillae. (C) Left and right spicules. (D) Uterus with four uterine branches. Scale bars: (A, C) 100 µm; (B, D) 50 µm.

generated topologies and the permutation tail probability (PTP) test (Faith & Cranston, 1991), with 10,000 permutations. Both tests were implemented using PAUP*.

Results

Systematics

Superfamily: Physalopteroidea Sobole, 1949
Family: Physalopteridae Leiper, 1908
Subfamily: Physalopterinae Railliet, 1893
Genus: *Physaloptera* Rudolphi, 1819
***Physaloptera amazonica* n. sp.**

Description

Body robust, filiform with fine transversal cuticular striations along the body. Sexual dimorphism present, females more robust than males. Anterior end forming cephalic collarette (figs 1a and 2a). Oral opening with two semi-circular pseudolabia presenting an external lateral tooth with a triangular shape, and three internal lateral teeth forming a tripartite structure on each side (fig. 3a, b). Apical region presenting two pairs of papillae, porous area and one pair of amphids (fig. 3a). Three well-delimited porous areas present on each lip (fig. 3a). Oesophagus divided into anterior muscular and posterior glandular parts (fig. 1a). Nerve ring surrounding the middle portion of muscular oesophagus. Excretory pore located in the first third of the body (fig. 1a).

Males. Based on holotype and seven paratypes. Total body length 27.86 (22.80–31.20); width at mid-body 1.26 (0.89–1.70). Muscular and glandular oesophagus 0.56 (0.50–0.69) and 2.85 (1.91–4.43) long, respectively. Nerve ring and excretory pore 0.62 (0.32–0.71) and 1.03(0.86–1.52) from the anterior end, respectively (figs 1a and 2a). Posterior end ventrally curved, with caudal alae ornate with irregular longitudinal ridges. Twenty-one caudal papillae: four pairs of pedunculated subventral

https://doi.org/10.1017/S0022149X19000610 Published online by Cambridge University Press

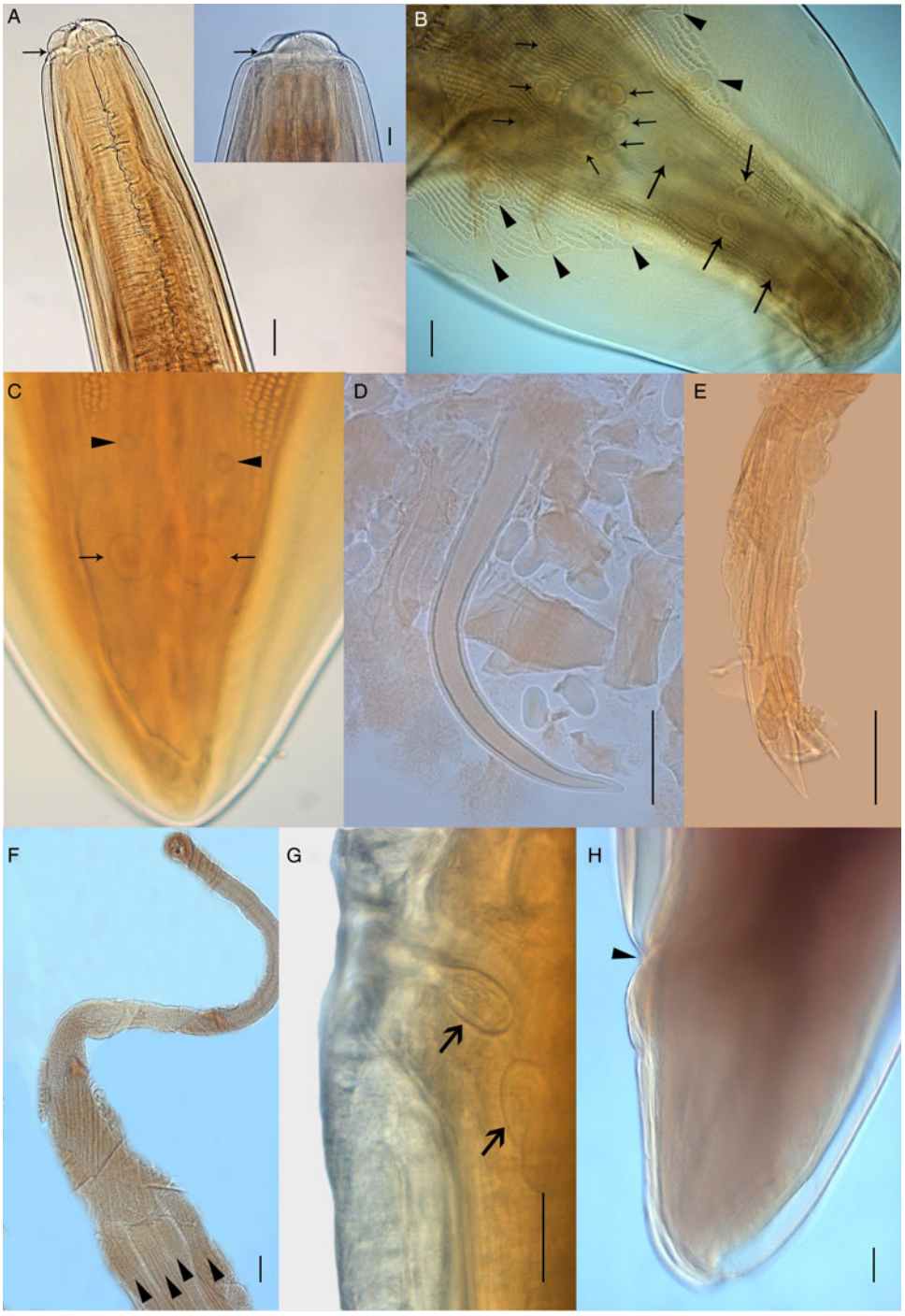

Fig. 2. Light microscopy of *Physaloptera amazonica* n. sp. (A) Male, ventral view, anterior end showing cephalic collarette and nerve ring (arrow). Detail showing tripartite tooth (scale bar: 50 µm). (B) Male, ventral view, posterior end showing pedunculated papillae (arrowheads) and sessile papillae (arrows). (C) Male, ventral view, posterior end showing phasmids (arrowheads) and pair of papillae (arrows). (D) Right spicule. (E) Left spicule. (F) Uterus with four uterine branches (arrowheads). (G) Vulva opening showing eggs, lateral view. (H) Female, lateral view, posterior end showing anus. Scale bars: (A, F, H) 100 µm; (B, C, D, E, G) 50 µm.

papillae; one pair of subventral, precloacal, sessile papillae and bigger, ventral, median unpaired one; two pairs of sessile papillae immediately posterior to cloacal opening and three pairs of postcloacal papillae: first and second pairs asymmetrically displaced, left one anterior to right one. Third pair of postcloacal papillae equidistant near the caudal end. Presence of a pair of phasmids between the second and third pairs of postcloacal papillae (figs 1b and 2b, c). Spicules sub-equal and different in shape, right one curved without dilatation, 0.45 (0.40–0.50) long (figs 1c and 2d), and left one lanceolate at the final third 0.51 (0.42–0.63) long (figs 1c and 2e), representing 1.58–1.73% and 1.82–2.32% of total body length (SpL/BL), respectively.

Females. Based on allotype and nine paratypes. Total body length 37.71 (22.50–63.00) and width at mid-body 1.55 (0.87–3.00). Muscular and glandular oesophagus 0.67 (0.44–0.91) and 3.34 (2.21–4.02), respectively. Nerve ring and excretory pore

https://doi.org/10.1017/S0022149X19000610 Published online by Cambridge University Press

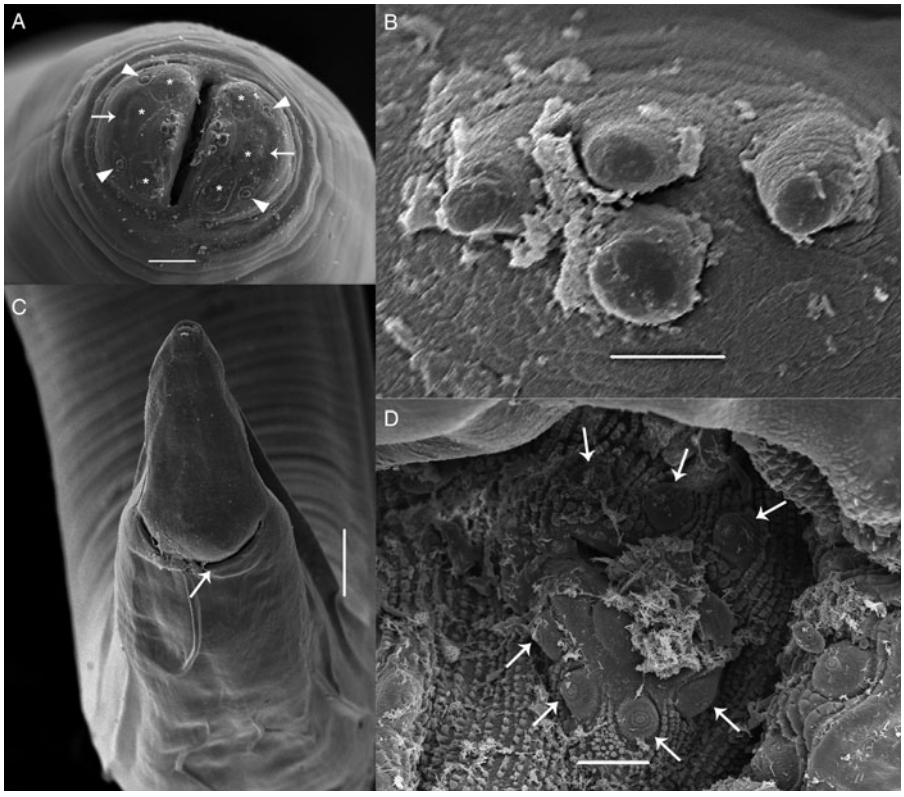

Fig. 3. Scanning electron microscopy of *Physaloptera amazonica* n. sp. (A) Female, apical view, anterior end showing pseudolabia with cephalic papillae (arrowheads), tripartite and small teeth, amphid (arrows), porous areas (*). (B) External lateral tooth and internal lateral tripartite teeth. (C) Female, ventral view, posterior end, showing the anal opening (arrow) and phasmids (arrowhead). (D) Transversal section showing uterus with eggs (arrowhead) and larvae at first stage (arrow). Scale bars: (A) 50 µm; (B) 10 µm; (C) 200 µm; (D) 20 µm.

0.35 (0.11–0.43) and 1.66 (1.14–12.70) from anterior end, respectively. Uterus with four uterine branches (figs 1d and 2f). Vulva opening 13.84 (6.11–23.62) from the anterior end (fig. 2g). Slit-like anal opening 0.92 (0.51–1.22) from the posterior end (figs 2h and 3c). Tail conical. Eggs elliptical 0.05 (0.05) long and 0.03 (0.02–0.03) wide with a thick and hyaline wall (fig. 2g).

Taxonomic summary

Type host. Proechimys gardneri (da Silva, 1998) (Rodentia: Echimyidae).

Site of infection. Stomach.

Type locality. Municipality of Xapuri, state of Acre, Brazil (10° 49′S, 68°21′W).

Prevalence. 15.6% (five rodents infected/32 rodents collected).

Mean intensity. 9 (1–19 per host).

Specimens deposited. Holotype: CHIOC 38715 (male); allotype: CHIOC 38720a (female); paratypes: CHIOC 38720b (one male and one female). All specimens were in wet materials.

Etymology. The specific epithet name refers to the biome where the hosts were collected.

Molecular and phylogenetic analyses

The 18S gene matrix had 22 taxa and 820 characters, of which 681 were constant, 79 were parsimony-uninformative variable and 60 were parsimony-informative variable (supplementary file S1). The MT-CO1 gene matrix had 20 taxa and 708 characters, of which 344 were constant, 122 were parsimony-uninformative variable and 242 were parsimony-informative variable (supplementary file S2). Both the PTP test and the g1 statistic indicated a strong phylogenetic signal in all datasets (supplementary file S3). Xia's test (Xia, 2018) provided evidence of substantial saturation only at the third codon positions in the MT-CO1 dataset (supplementary file S4).

MP heuristic searches resulted in two most-parsimonious trees for the 18S matrix (scores = 202 steps; consistency indexes = 0.8020; supplementary file S1) and a single most-parsimonious tree for the MT-CO1 matrix (score = 960 steps; consistency index = 0.5687; supplementary file S2).

As the best-fit model for the 18S matrix, PAUP* selected GTR + I + G, with estimated frequencies, rates, Gamma (0.7139) and invariable sites (0.6558). The best log-likelihood ML-tree score for 18S was −2055.797 (supplementary file S5). As the best-fit model for the MT-CO1 matrix, PAUP* selected GTR + I + G, with estimated frequencies, rates, Gamma (0.3285) and invariable sites (0.3096). The best log-likelihood ML-tree score for MT-CO1 was −4626.594 (supplementary file S6).

For the BIs, at the 18S matrix, the mean estimated marginal likelihood was −2091.5880 and the median was −2091.2380 (supplementary file S7); at the MT-CO1 matrix, the mean estimated marginal likelihood was −4174.9832 and the median was −4174.6310 (supplementary file S8); ESSs for all parameters were above 100 effectively independent samples and much larger for most parameters, demonstrating the robustness of our sampling for both matrices (supplementary files S7 and S8).

The 18S matrix had pairwise interspecific genetic *p*-distances (supplementary file S9) ranging from zero between *Physaloptera bispiculata* and *Physaloptera* sp. from Costa Rica, and between *P. mirandai* and *P. galvaoi* to 10.9% between *G. turgidum* and *P. galvaoi*. Intraspecific genetic distances in the 18S matrix ranged from zero within *P. mirandai* and *Turgida turgida* to 0.2% within *Heliconema longissimum*. Distances of *P. amazonica* n. sp. ranged

https://doi.org/10.1017/S0022149X19000610 Published online by Cambridge University Press

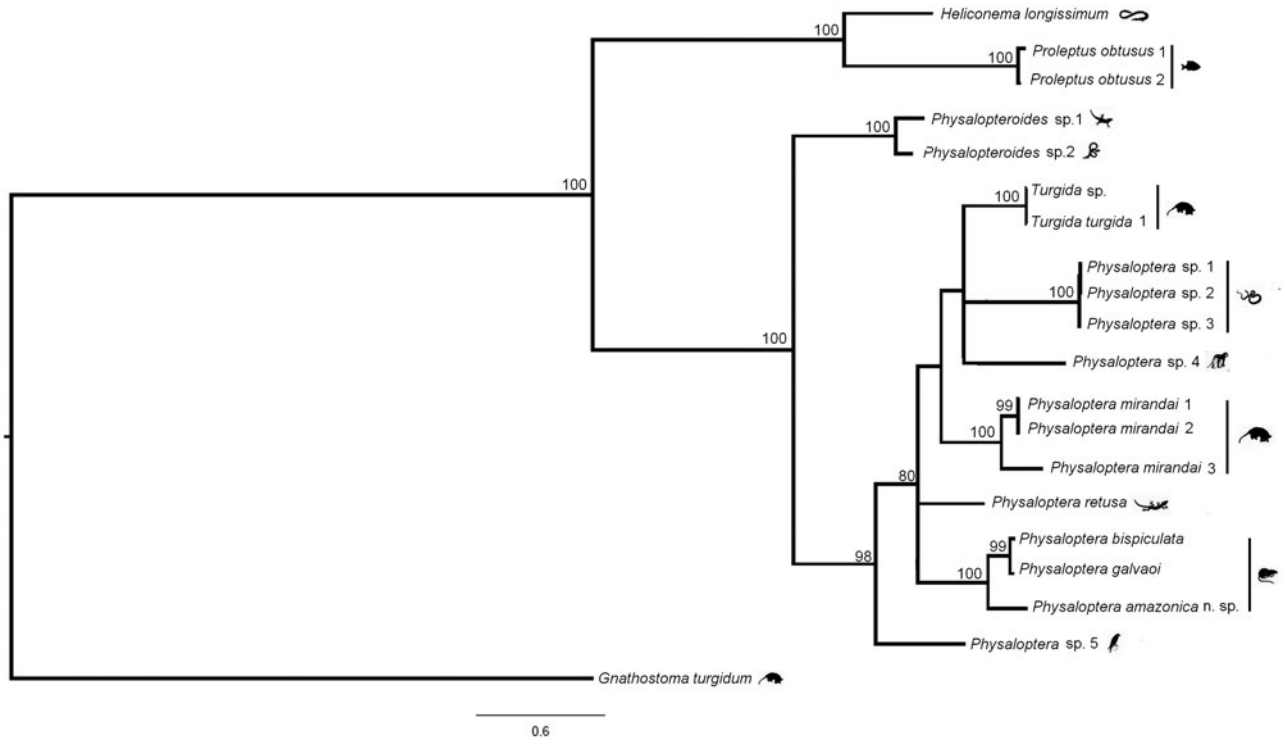

Fig. 4. Phylogenetic relationships of Physalopteridae based on the MT-CO1 gene generated by Bayesian inference. Values of Bayesian posterior probabilities are on the tree nodes. The scale bar represents the number of substitutions per site.

from 0.1% (*P. mirandai* and *P. galvaoi*) to 0.2% (*Physaloptera* sp. from Costa Rica), 0.3% (*P. bispiculata*), 0.5–0.6% (*T. turgida*), 0.9% (*Physaloptera* sp., from China), 1.0% (*P. rara*, *Physaloptera* sp. from USA and *T. torresi*), 1.8% (*P. apivori*), 1.9% (*P. alata*), 2.1% (*P. thalacomys*), 3.0% (*Physalopteroides* sp.), 3.8–3.9% (*H. longissimum*), 3.9% (*P. obtusus*), 4.4% (*Proleptus* sp.) and 10.4% (*G. turgidum*).

The MT-CO1 matrix had pairwise interspecific genetic *p*-distances (supplementary file S10) ranging from 3.4% between *P. bispiculata* and *P. galvaoi* to 35.6% between *G. turgidum* and *P. obtusus*. Intraspecific genetic distances in the MT-CO1 matrix ranged from zero within *P. mirandai*, *Physaloptera* sp. from Mexico and *T. turgida* to 9.3% within *P. mirandai*. Distances of *P. amazonica* n. sp. ranged from 9.7% (*P. galvaoi*) to 9.9% (*P. bispiculata*), 13.0% (*P. retusa*), 13.4–14.1% (*P. mirandai*), 13.8% (*Physaloptera* sp. from USA), 13.9% (*T. turgida*), 14.9–15.1% (*Physaloptera* sp. from Mexico), 15.3% (*Physaloptera* sp. from Costa Rica), 18.9–19.3% (Physalopteridae gen sp. 1 and Physalopteridae gen sp. 2), 22.5% (*H. longissimum*), 22.3–23.3% (*P. obtusus*) and 32.7% (*G. turgidum*).

Phylogenetic trees produced with different datasets were poorly resolved, with few strongly supported branches, regardless of the inference method used. Consistent similarities were found mostly involving moderately to well-supported branches (supplementary files S11–S18). *Heliconema* and *Proleptus* species sequences formed a poorly to well-supported monophyletic group in all phylogenies using either 18S (MP-BS = 0.79; ML-SH = 0.67; BPP = 0.90) or MT-CO1 (MP-BS = 1.00; ML-SH = 0.99; BPP = 1.00) matrices (fig. 4 and 5).

Physalopterinae species sequences formed a moderately to well-supported monophyletic group in all phylogenies using either 18S (MP-BS = 0.75; ML-SH = 0.94; BPP = 0.99) or MT-CO1 (MP-BS = 1.00; ML-SH = 0.98; BPP = 1.00). Relationships within Physalopterinae were poorly resolved and most species were connected with polytomies or weakly supported branches. *Turgida* species sequences formed a poorly to well-supported monophyletic group in all phylogenies using either 18S (MP-BS < 0.50; ML-SH = 0.79; BPP = n/a) or MT-CO1 (MP-BS = 1.00; ML-SH < 0.50; BPP = 1.00), except for the BI-18S tree. Moreover, *Turgida* consistently nested within clades formed by *Physaloptera* species sequences, making *Physaloptera* paraphyletic in all phylogenies, using both matrices.

Regarding exclusively the 18S matrix, *P. alata* and *P. apivori* sequences formed a well-supported monophyletic group in all phylogenies (MP-BS = 0.97; ML-SH = 0.97; BPP = 1.00), whereas *P. rara*, *P. thalacomys* and *Physaloptera* sp. from USA sequences formed a poorly to well-supported monophyletic group in all but the BI tree (MP-BS < 0.50; ML-SH = 0.92; BPP = n/a).

Regarding exclusively the MT-CO1 matrix, *P. mirandai* sequences formed a well-supported monophyletic group in all phylogenies (MP-BS = 0.81; ML-SH = 1.00; BPP = 1.00), whereas *P. bispiculata* and *P. galvaoi* sequences both formed a well-supported monophyletic group in all phylogenies (MP-BS = 1.00; ML-SH = 0.98; BPP = 0.99).

Physaloptera amazonica n. sp. did not consistently cluster with other species in the 18S matrix. Instead, it sometimes grouped with *Turgida* species, *Physaloptera* sp. from China, *Physaloptera* sp. from Costa Rica, *P. mirandai*, *P. bispiculata* and *P. galvaoi* in a poorly resolved and poorly to moderately supported monophyletic group in all but the BI tree (MP-BS < 0.50; ML-SH = 0.84; BPP = n/a); or grouped with *P. alata* and *P. apivori*, *P. bispiculata*, *P. galvaoi*, *P. mirandai*, *Physaloptera* sp. from China, *Physaloptera* sp. from Costa Rica, *Physalopteroides* sp. and *Turgida* in a poorly resolved, well-supported monophyletic

https://doi.org/10.1017/S0022149X19000610 Published online by Cambridge University Press

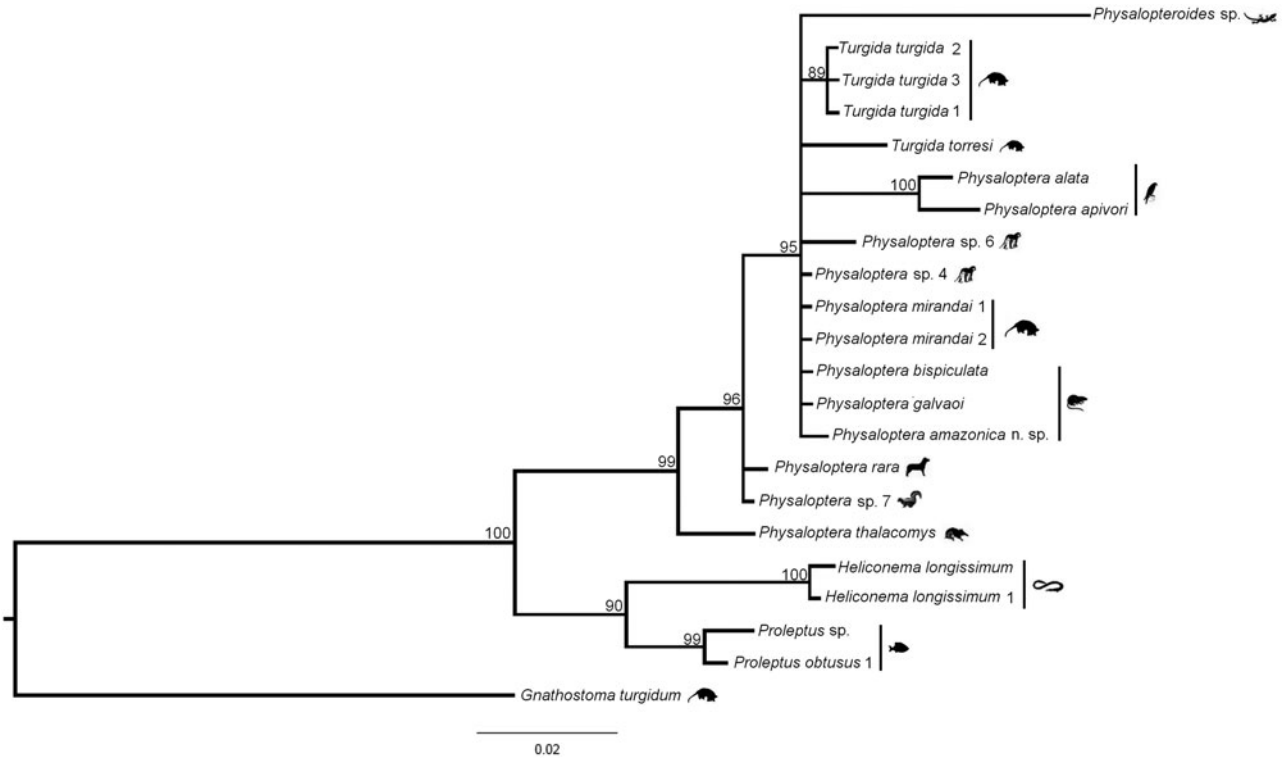

Fig. 5. Phylogenetic relationships of Physalopteridae based on the nuclear ribosomal RNA small subunit (18S) gene generated by maximum likelihood. Values of local support values using the Shimodaira–Hasegawa test with 1000 resamples are on the tree nodes. The scale bar represents the number of substitutions per site.

group in the BI consensus tree (BPP = 0.95). In the MT-CO1 matrix, *P. amazonica* n. sp. formed a well-supported monophyletic group with the *P. bispiculata* + *P. galvaoi* clade in all phylogenies (MP-BS = 0.98; ML-SH = 1.00; BPP = 1.00).

Discussion

The new species presented here belongs to the genus *Physaloptera* due to the following morphological features: cuticle forming a cephalic collarette at anterior end, two pseudolabia surrounding the oral opening with one external lateral tooth and internal lateral tripartite tooth, males with caudal alae well-developed presenting papillae (four lateral pedunculated pairs, three precloacal and five sessile postcloacal pairs), spicules sub-equal, females presenting vulva at the anterior third of the body and less than ten uterine branches (Travassos, 1920; Ortlepp, 1922; Morgan, 1947).

Comparing *P. amazonica* n. sp. with the species described in rodents from the Americas, it can be distinguished from *P. longispicula* Quentin, 1968, *P. murisbrasiliensis* Diesing, 1860, *P. calnuensis* Sutton, 1989 and *P. bispiculata* Vaz & Pereira, 1935 by having the first and second pair of sessile papillae asymmetrically organized, with the left one anterior to the right one. The new species differs from all *Physaloptera* parasites from American rodents by the spicule shape – that is, right one curved without dilatation and left one lanceolate at the final third. Moreover, the ratio of left spicule/total body length of *P. amazonica* n. sp. is larger than those of *P. goytaca* Ederli, Gallo, Oliveira & Oliveira, 2018, *P. galvaoi* São Luiz, Simões, Torres, Barbosa, Santos, Giese, Rocha & Maldonado Júnior, 2015, *P. hispida* Schell, 1950 and *P. murisbrasiliensis*. The position of the excretory pore from the anterior end in *P. amazonica* n. sp. is larger than in *P. calnuensis* and *P. longispicula*, both in male and female specimens. The number of uterine branches from the present species differs from *P. hispida*, *P. bispiculata*, *P. murisbrasiliensis* and *P. goytaca* by having four branches. The distance of vulva from the anterior end of the new species is larger than in *P. bispiculata* and *P. calnuensis* (table 2).

Currently, five species of *Physaloptera* infecting rodents have been reported, found in different biomes in Brazil: *P. bispiculata* parasitizing *Nectomys squamipes* Brants, 1827 and *P. murisbrasiliensis* in *Holochilus brasiliensis* (Desmarest, 1819) (syn. *Mus brasiliensis*), both in the Atlantic Rainforest; *P. longispicula* in *Thrichomys apereoides* (Lund, 1839) in Caatinga; *P. galvaoi* in *Cerradomys subflavus* (Wagner, 1842) in Cerrado; and *P. goytaca* in *C. goytaca* in Restinga (sandplain) (Ortlepp, 1922; Morgan, 1947; Vicente *et al.*, 1997; São Luiz *et al.*, 2015; Ederli *et al.*, 2018). In this study, *P. amazonica* n sp. represents the only species infecting an echimyid rodent in the Amazon forest.

Our phylogenetic analyses were inconclusive in some respects due to several reasons, as follows. (1) Insufficient taxonomic coverage: since *Physaloptera* is such a speciose genus, our datasets represented less than 10% of the total number of species recognized for the genus. (2) Taxonomic uncertainties: several sequences in each of our datasets have not been identified at the species level, some have not even been identified at the genus level. Moreover, there may be cryptic species of *Physaloptera* yet undetected. Finally, there is the issue of taxonomic reliability of DNA sequences in public sequence databases, which sometimes are not sufficiently complete or do not contain correctly and informatively annotated entries. Indeed, up to 20% of the named sequences in public databases may be misidentified

https://doi.org/10.1017/S0022149X19000610 Published online by Cambridge University Press

Table 2. Morphological features of *Physaloptera* males/females infecting rodents in the Americas.

	Physaloptera amazonica n. sp. Present study		*Physaloptera goytaca* Ederli, Gallo, Oliveira & de Oliveira, 2018		*Physaloptera galvaoi* São Luiz, Simões, Torres, Barbosa, Santos, Giese, Rocha & Arnaldo Maldonado Júnior, 2015		*Physaloptera calnuensis* Sutton, 1989		*Physaloptera longispicula* Quentin, 1968		*Physaloptera bispiculata* Vaz & Pereira, 1935		*Physaloptera hispida* Schell, 1950		*Physaloptera murisbrasiliensis* Diesing, 1860	
	Male	Female	Male	Female	Male	Female	Male	Female	Male	Female	Male	Female	Male	Female	Male	Female
Total body length	22.80–31.20	22.50–63.00	19.00–27.00	25.90–58.17	10.00–23.00	16.40–31.30	17.10	28.07	34.40	15.28–30.41	25.00	27.00–55.00	30.00–42.00	53.00–64.00	22.00–28.00	35.00–43.00
Body width	0.89–1.70	0.87–3.00	0.80–1.20	0.99–1.85	0.80–0.90	1.10–3.18	0.61	0.99	1.40	0.40–0.57	0.80	1.00–1.90	0.90–1.40	1.90–2.00	0.87–0.95	1.10–1.75
Muscular oesophagus length	0.50–0.69	0.44–0.91	0.39–0.61	0.37–0.66	0.46–0.58	0.42–0.66	0.33	0.39	0.60	0.25–0.40	0.50	0.54–0.70	0.56–0.73	0.64–0.69	–	–
Glandular oesophagus length	1.91–4.43	2.21–4.02	2.40–3.60	3.20–7.30	3.00–3.74	1.27–4.14	2.99	3.32	5.30	2.70–3.76	3.20	3.80–5.40	3.70–4.50	3.80–5.40	–	–
Nerve ring	0.32–0.71	0.11–0.43	0.42–0.64	0.35–0.77	0.20–0.43	0.20–0.28	0.34–0.41	0.38	0.50	0.26–0.40	–	–	0.55–0.70	0.71–0.74	–	–
Excretory pore	0.86–1.52	1.14–2.70	0.77–0.86	0.59–1.52	0.52–0.95	0.68–1.66	0.80	0.78	0.83	0.36–0.56	–	1.20	0.87–1.20	0.84–1.08	–	–
Cloaca[a]	1.12–1.31	0.51–1.22	0.48–0.75	0.41–0.80	0.28–0.61	0.43–0.50	0.58	0.52	1.90	0.20–0.61	0.87	–	–	–	–	–
Right spicule	0.40–0.50	–	0.19–0.23	–	0.19–0.23	–	0.31	–	0.71	–	0.40	–	0.39–0.55	–	0.40	–
RSp/BL	1.58–1.73%	–	1.60%	–	1.29%	–	1.81%	–	2.06%	–	1.6%	–	1.57%	–	1.6%	–
Left spicule	0.42–0.63	–	0.32–0.45	–	0.23–0.28	–	0.42	–	0.85	–	0.46	–	0.23–0.28	–	0.40	–
LSp/BL	1.82–2.32%	–	1.63%	–	1.13%	–	2.45%	–	2.47%	–	1.84%	–	1.27%	–	1.6%	–
Vulva[b]	–	6.11–23.62		7.20–19.08	–	6.42–11.14	–	12.28	–	9.35–19.46		10.2–13.2		11.00–16.00	–	–
Eggs	–	0.05–0.02		0.05 × 0.02	–	0.05 × 0.03	–	0.04 × 0.02	–	0.06 × 0.04		0.05 × 0.04		0.05 × 0.04	–	0.05 × 0.03
Uterine branches	–	4		5	–	4–5	–	–	–	–		2		2	–	2
Host	*Proechimys gardneri*		*Cerradomys goytaca*		*Cerradomys subflavus*		*Calomys laucha*		*Thrichomys apereoides* (= *Cercomys cunicularius*)		*Nectomys squamipes*		*Sigmodon hispidus*		*Mus brasiliensis* (= *Holochilus brasiliens)*	
Locality	Brazil		Brazil		Brazil		Uruguay		Brazil		Brazil		USA		Brazil	

All measurements are in millimetres.
[a]Distance from posterior end.
[b]Distance from anterior end.
RSp/BL and LSp/BL = ratio of right spicule/body total length or left spicule/body total length.

(Vilgalys, 2003; Nilsson *et al.*, 2006). (3) Unbalanced taxonomic representativeness between matrices: not all taxa were represented in both matrices. (4) Molecular markers' evolutionary rates: MT-CO1 performs better at species-level differentiation, while 18S is more adequate at deeper nodes. However, MT-CO1 evolves faster and is more inclined to saturation, whereas 18S evolves slower, has a larger effective population size and is more inclined to incomplete lineage sorting. Therefore, including a third marker, with intermediate mutational rates, such as the ITS region, would provide a more complete perspective on the relationships between species of *Physaloptera* and genera of physalopterids. (5) Inference methods consistency: during analyses, we noticed that divergence levels and saturation were relatively low, even for the MT-CO1, although heterogeneous. In such situations, MP may perform better than probabilistic methods due to overparameterization (Russo *et al.*, 1996; Kolaczkowski & Thornton, 2004) and lack of gap treatment of the last, particularly when there are gaps in the matrix (e.g. the 18S), which are treated as a fifth state in MP (Warnow, 2012). Indeed, we found more congruence between MP and ML than between ML and BI, in both matrices, suggesting inconsistency of the statistical methods for our data.

Relationships between most taxa within *Physaloptera* were poorly resolved in our phylogenies, producing multifurcations or a star phylogeny. Star-like phylogenetic patterns have been observed for different taxa, from viruses to vertebrates (Leite & Patton, 2002; Castillo *et al.*, 2005; Almeida *et al.*, 2011; Poon *et al.*, 2013), and may occur due to poor taxonomic sampling or lack of phylogenetic signal, either because of saturation in variable genes (such as the MT-CO1) or because of insufficient mutations in conserved genes (such as the 18S). Although both genes have very different mutation rates, as was demonstrated by our distance matrices, we found little saturation in most datasets, except for the third codon positions in the MT-CO1, and a strong phylogenetic signal conveyed by all datasets. Finally, the star-like pattern may be attributed to evolutionary processes where past simultaneous species diversification events took place. Explosive speciation processes in parasites may be a result of new host capture in a short span, enabling rapidly diverging lineages to persist over time, leading to short branches near the root and long branches at the tips. This is a reasonable conjecture for *Physaloptera*, considering that species are found infecting marsupials, rodents, reptiles, amphibians and birds (Honisch & Krone, 2008; Humberg *et al.*, 2011; Pereira *et al.*, 2012; Quadros *et al.*, 2014).

Despite all uncertainties concerning the phylogenies, there was a consensus, in our molecular analyses, that *P. amazonica* n. sp. belongs to a lineage independent of the other species of *Physaloptera* and should, therefore, be considered a separate species. Both pairwise genetic distances and phylogenetic trees approximated *P. amazonica* n. sp. to other Neotropical species, notably *P. bispiculata* and *P. galvaoi*.

Our phylogenetic analyses also showed *Turgida* consistently forming a monophyletic group, although not always well-supported. This group nested within *Physaloptera*, which was, therefore, paraphyletic, suggesting that *Turgida* may have evolved from a *Physaloptera*-like monodelphic ancestor and could be a derived form of *Physaloptera*, as pointed out by Ortlepp (1922), stressing that polydelphy is a common trait among several species within both genera. Likewise, morphological diagnostic differences between *Physaloptera* and *Turgida* are inconsistent, so the use of morphological differences such as the number of uterus branches, pattern of caudal papillae arrangement, spicule size and shape should be viewed carefully and considered with caution, as it could also be the case that some species classified as *Physaloptera* really belong to other genera.

In conclusion, *P. amazonica* n. sp. is distinguished from other species of the genus by morphological and molecular evidence, emphasizing the importance of integrative taxonomy in supporting systematic studies of nematodes. Due to the great diversity of *Physaloptera*, further analyses should include more taxa, particularly the polydelphic ones, and more molecular markers for all taxa to elucidate the underlying evolutionary history between species of *Physaloptera* and genera of physalopterids.

Supplementary material. To view supplementary material for this article, please visit https://doi.org/10.1017/S0022149X19000610.

Acknowledgements. We thank the staff of the Laboratory for Biology and Parasitology of Wild Mammal Reservoirs of IOC/Fiocruz, Brazil, for helping in the field work, and Ricardo Baptista Schmidt of the Image Production and Treatment Service, IOC/Fiocruz,.

Financial support. AMJ received a grant from the National Council for Scientific and Technological Development – CNPq (grant number 306352/2014-1). ROS received a grant from the Rio de Janeiro State Research Foundation – FAPERJ (grant number E-26/202.128/2015).

Conflicts of interest. None.

Ethical standards. Animals were captured under the authorization of the Brazilian government's Chico Mendes Institute for Biodiversity and Conservation (ICMBIO, license number 13373, 45839-2, 17131-4), the Santa Catarina State Environmental Foundation (FATMA, license number 043/2014) and the Rio de Janeiro State Environmental Institute (INEA-020/2011). All procedures followed the guidelines for capture, handling and care of animals of the Ethical Committee on Animal Use of the Oswaldo Cruz Foundation (CEUA FIOCRUZ license number 066/08; L-049/08, LW81/12 and 39/14, CEUA UESC-003/2013).

References

Abascal F, Zardoya R and Telford MJ (2010) TranslatorX: Multiple alignment of nucleotide sequences guided by amino acid translations. *Nucleic Acids Research* **38**, w7–13.

Almeida FC, Giannini NP, DeSalle R and Simmons NB (2011) Evolutionary relationships of the old world fruit bats (Chiroptera, Pteropodidae): Another star phylogeny? *BMC Evolutionary Biology* **11**, 281.

Anderson RC, Chabaud AG and Willmott S (2009) *Keys to the nematode parasites of vertebrates. Archival volume*. 463 pp. Wallingford, UK, CABI Publishing.

Castillo AH, Cortinas MN and Lessa EP (2005) Rapid diversification of South American Tuco-Tucos (Ctenomys; Rodentia, Ctenomyidae): Contrasting mitochondrial and nuclear intron sequences. *Journal of Mammalogy* **86**, 170–179.

Chabaud AG (1975) Keys to genera of the Order Spirurida. pp. 1–27 in Anderson RC, Chabaud AG, Wilmont S (Eds) *CHI keys to the nematode parasites of vertebrates*. United Kingdom, Commonweal.

Ederli NB, Gallo SSM, Oliveira LC and de Oliveira FCR (2018) Description of a new species *Physaloptera goytaca* n. sp. (Nematoda, Physalopteridae) from *Cerradomys goytaca* Tavares, Pessôa & Gonçalves, 2011 (Rodentia, Cricetidae) from Brazil. *Parasitology Research* **117**, 2757–2766.

Edgard RC (2004) MUSCLE: Multiple sequence alignment with high accuracy and high throughput. *Nucleic Acids Research* **32**, 1792–1797.

Eler ES, Da Silva MNF, Silva CEF and Feldberg E (2012) Comparative cytogenetics of spiny rats of the genus *Proechimys* (Rodentia, Echimyidae) from the Amazon region. *Genetics and Molecular Research* **11**, 830–846.

Emmons LH and Feer F (1997) *Neotropical rainforest mammals. A field guide*. 2nd edn. 396 pp. Chicago, University of Chicago Press.

Faith DP and Cranston PS (1991) Could a cladogram this short have arisen by chance alone?: On permutation tests for cladistic structure. *Cladistics* **7**, 1–28.

Galewski T, Mauvrey JF, Leite YLR, Patton JL and Douzery EJP (2005) Ecomorphological diversification among South American spiny rats (Rodentia; Echimyidae): a phylogenetic and chronological approach. *Molecular Phylogenetics Evolution* **34**, 601–615.

Gannon WL and Sikes RS (2011) Guidelines of the American Society of Mammalogists for the use of wild mammals in research. *Journal of Mammalogy* **92**, 235–253.

Goldberg SR and Bursey CR (2002) Gastrointestinal helminths of seven gekkonid lizard species (Sauria: Gekkonidae) from Oceania. *Journal of Natural History* **36**, 2249–2264.

Hobmaier M (1941) Extramammalian phase of *Physaloptera maxillaris* Molin, 1860 (Nematoda). *Journal of Parasitology* **27**, 233.

Honisch M and Krone O (2008) Phylogenetic relationships of Spiruromorpha from birds of prey based on 18S rDNA. *Journal of Helminthology* **82**, 129–33.

Humberg RMP, Tavares LER, Paiva F, Oshiro ET, Bonamigo RA, Júnior NT and Oliveira AG (2011) *Turgida turgida* (Nematoda: Physalopteridae) parasitic in white-bellied opossum, *Didelphis albiventris* (Marsupialia: Didelphidae), state of Mato Grosso do Sul, Brazil. *Pesquisa Veterinária Brasileira* **31**, 78–80.

Kearse M, Moir R, Wilson A, Stones-Havas S, Cheung M, Sturrock S, Buxton S, Cooper A, Markowitz S, Duran C, Thierer T, Ashton B, Meintjes P and Drummond A (2012) Geneious Basic: an integrated and extendable desktop software platform for the organization and analysis of sequence data. *Bioinformatics* **28**, 1647–1649.

Kolaczkowski B and Thornton JW (2004) Performance of maximum parsimony and likelihood phylogenetics when evolution is heterogeneous. *Nature* **431**, 980–984.

Leite YLR and Patton JL (2002) Evolution of South American spiny rats (Rodentia, Echimyidae): The star-phylogeny hypothesis revisited. *Molecular Phylogenetics and Evolution* **25**, 455–464.

Maddison WP and Maddison DR (2018), Mesquite: A modular system for evolutionary analysis. Version 1.0. http://www.mesquiteproject.org.

Migueis R (2001) *Uma introdução à geografia do Amazonas*. 132 pp. Boa Vista, Gráfica Real.

Miller MA, Pfeiffer W and Schwartz T (2010) *Creating the CIPRES Science Gateway for inference of large phylogenetic trees*. In 2010 Gateway Computing Environments Workshop, (GCE), 14 November 2010. New Orleans, Louisiana, pp. 1–8.

Morgan BB (1947) Host-parasite relationships and geographical distribution of the *Physaloptera* (Nematode). *Transaction Wisconsin Academy Sciences, Arts and Letters Illinois* **38**, 273–292.

Nilsson RH, Ryberg M, Kristiansson E, Abarenkov K, Larsson KH and Kõljalg U (2006) Taxonomic reliability of DNA sequences in public sequence databases: A fungal perspective. *PLoS One* **1**, e59.

Ortlepp RJ (1922) The nematode genus *Physaloptera* Rudolphi, 1819. *Proceedings of the Zoological Society of London* **92**, 999–1107.

Panti-May JA, Hernández-Betancourt SF, Rodríguez-Vivas RI and Robles MR (2015) Infection levels of intestinal helminths in two commensal rodent species from rural households in Yucatan, Mexico. *Journal of Helminthology* **89**, 42–48.

Patton J and Leite Y (2015) Genus Proechimys J.A. Allen, 1899. pp. 950–988 *in* Patton JL, Pardiñas UF, D'Elía G (Eds) *Mammals of South America. vol. 2. Rodents*. Chicago, University of Chicago Press.

Pereira FB, Alves PV, Rocha BM, Lima SS and Luque JL (2012) A new *Physaloptera* (Nematoda: Physalopteridae) parasite of *Tupinambis merianae* (Squamata: Teiidae) from southeastern Brazil. *Journal of Parasitology* **98**, 1227–1123.

Pereira FB, Alves PV, Rocha BM, Lima SS and Luque JL (2014) *Physaloptera bainae* n. sp. (Nematoda: Physalopteridae) parasitic in *Salvator merianae* (Squamata: Teiidae), with a key to *Physaloptera* species parasitizing reptiles from Brazil. *Journal of Parasitology* **100**, 221–227.

Poon AFY, Walker LW, Murray H, McCloskey RM, Harrigan PR and Liang RH (2013) Mapping the shapes of phylogenetic trees from human and zoonotic RNA viruses. *PLoS One* **8**, e78122.

Portal Amazônia (2016) Amazônia de A a Z. *Epi Info*. Available at http://www.portalamazonia.com.br/secao/amazoniadeaz/interna.php?id=134 (accessed 10 November 2018).

Price MN, Dehal PS and Arkin AP (2010) FastTree 2 – Approximately maximum-likelihood trees for large alignments. *PLoS ONE* **5**, e9490.

Prosser SWJ, Velarde-Aguilar MG, León-Règagnon V and Hebert PDN (2013) Advancing nematode barcoding: a primer cocktail for the cytochrome c oxidase subunit I gene from vertebrate parasitic nematodes. *Molecular Ecology Resources* **13**, 1108–1115.

Pruesse E, Peplies J and Glöckner FO (2012) SINA: Accurate high-throughput multiple sequence alignment of ribosomal RNA genes. *Bioinformatics* **28**, 1823–1829.

Quadros RM, Marques SMT, Moura AB and Antonelli M (2014) First report of the nematode *Physaloptera praeputialis* parasitizing a jaguarandi. *Neotropical Biology and Conservation* **9**, 186–189.

Rambaut A, Drummond AJ, Xie D, Baele G and Suchard MA (2018) Posterior summarization in Bayesian phylogenetics using tracer 1.7. *Systematic Biology* **67**, 901–904.

Ronquist F, Teslenko M, Mark PVD, Ayres DL. , Darling A, Höhna S, Larget B, Liu L, Suchard MA and Huelsenbeck JP (2012) MrBayes 3.2: efficient Bayesian phylogenetic inference and model choice across a large model space. *Systematic Biology* **61**, 539–542.

Russo CAM, Takezaki N and Nei M (1996) Efficiencies of different genes and different tree-building methods in recovering a known vertebrate phylogeny. *Molecular Biology and Evolution* **13**, 525–536.

São Luiz J, Simões RO, Torres EL, Barbosa HS, Santos JN, Giese EG, Rocha FL and Maldonado Jr A (2015) A new species of *Physaloptera* (Nematoda: Physalopteridae) from *Cerradomys subflavus* (Rodentia: Sigmodontinae) in the Cerrado Biome, Brazil. *Neotropical Helminthology* **9**, 301–312.

Silva JMC, Rylands AB and Fonseca GAB (2005) The fate of the Amazonian areas of endemism. *Conservation Biology* **19**, 688–694.

Sokal RR and Rohlf FJ (1995) *Biometry: the principles and practice of statistics in biological research*. New York, W.H Freeman, p. 886.

Swofford DL (2002) *PAUP*. Phylogenetic Analysis Using Parsimony (*and Other Methods)*. Sunderland, MA, Sinauer Associates.

Travassos L (1920) Contribuições para o conhecimento da fauna helmintológica brasileira. X. Sobre as espécies do gênero *Turgida*. *Memórias do Instituto Oswaldo Cruz* **12**, 73–77.

Vicente JJ, Rodrigues HO, Gomes DC and Pinto RM (1997) Nematóides do Brasil. Parte V: Nematóides de mamíferos. *Revista Brasileira de Zoologia* **14**, 1–452.

Vilgalys R (2003) Taxonomic misidentification in public DNA databases. *New Phytologist* **160**, 4–5.

Warnow T (2012) Standard maximum likelihood analyses of alignments with gaps can be statistically inconsistent. *PLOS Currents* **4**, 1–14.

Xia X (2018) DAMBE7: New and improved tools for data analysis in molecular biology and evolution. *Molecular Phylogenetics and Evolution* **35**, 1550–1552.

Xia X and Lemey P (2009) Assessing substitution saturation with DAMBE. pp. 615–630 *in* Lemey P, Salemi M and Vandamme AM (*Eds*) *The phylogenetic handbook: A practical approach to phylogenetic analysis and hypothesis testing*. Cambridge, Cambridge University Press.

Xia X, Xie Z, Salemi M, Chen L and Wang M (2003) An index of substitution saturation and its application. *Molecular Phylogenetics and Evolution* **26**, 1–7.